

Data-driven control-oriented modelling for MPC-based control of urban drainage systems[★]

Luis Romero-Ben^{*} Bernat Joseph-Duran^{**} David Sunyer^{***}
 Gabriela Cembrano^{*} Jordi Meseguer^{**} Vicenç Puig^{*}
 Alejandro Carrasco^{****}

^{*} Institut de Robòtica i Informàtica Industrial, CSIC-UPC, Llorens i Artigas 4-6, 08028, Barcelona, Spain (e-mail: luis.romero.ben@upc.edu).

^{**} CETqua, Water Technology Centre, Ctra. d'Esplugues 75, 08940, Barcelona, Spain.

^{***} Area of Resilience and Climate Change. Aquatec S.L., Paseo de la Zona Franca 48, 08038, Barcelona, Spain.

^{****} Development Innovation Area. Canal de Isabel II, C/ Santa Engracia 125, 28003 Madrid, Spain.

Abstract: This article presents a data-driven, control-oriented modelling methodology for urban drainage systems (UDS). The proposed framework requires three main key components: input-output data from the element to be modelled, expert knowledge to define the model structure, and data-fitting techniques to obtain optimal parameters. The methodology is evaluated using a realistic benchmark from an UDS in Madrid, Spain. The results show high model accuracy and improved performance within a MPC scheme, reducing discharge and increasing treatment facilities utilization.

Keywords: urban drainage systems, data-driven modelling, model predictive control, water bodies protection, key performance indicators

1. INTRODUCTION

Nowadays, global population growth and expanding urbanization are altering the urban hydrological cycle, leading to increased combined sewer overflows (CSO) and stormwater discharge into water bodies (McGrane, 2016). The spilled water conveys pollutants like suspended solids (SS), hydrocarbons or heavy metals leading to a estimated 80% of the total volume returning to the water bodies to be polluted (UN-Water, 2017). The most effective approach to address this challenge is the advancement in urban drainage systems (UDS) management, which transport waste and stormwater to wastewater treatment plants (WWTP) for purification before release. This management can be enhanced through efficient control strategies such as real-time control (RTC), which iteratively monitor the system conditions and operate the actuators accordingly.

Early solutions relied on heuristic algorithms, based on the experience and intuition of network operators. The most common technique is rule-based control (RBC), which applies pre-defined rules to determine control actions under various scenarios (Aulinas et al., 2011). More recently, machine learning methods such as deep reinforcement learning (RL) have been exploited to develop controllers that

learn from experience (Mullapudi et al., 2020). Although these approaches can be effective, the former require of extremely detailed expert knowledge and the latter can be computationally expensive during training.

Between the development of heuristic and learning-based methods, optimization-based methods appeared as a reliable and effective solution. They use optimization algorithms and mathematical models of the UDS to minimize a certain cost function. Methods such as model predictive control (MPC) (Joseph-Duran et al., 2015) generally achieve excellent performance, but their applicability to real networks may be limited by the complexity of real-world UDS and the associated mathematical models, as well as potential modelling errors and uncertainty. While detailed dynamic models of UDS hydrodynamics are available for urban drainage simulation, simpler but representative models of the systems dynamics are required for optimization-based RTC, as the optimization process requires numerous computations of the outcomes of possible control actions within a control interval of a few minutes.

In this context, this article addresses the control-oriented modelling of UDS in the context of MPC-based methods. The paper presents several contributions:

- A methodology to derive data-based equations that approximate the behaviour of complex network elements is presented. Moreover, it is extended for the

[★] The authors wish to acknowledge the support from the European Commission research grant of project LIFE RUBIES (LIFE20 ENV/FR/000179). This work has been submitted to IFAC for possible publication

design of flow-setpoint curves that allow to retrieve the actuator setpoints from their associated flows.

- The validation of the methodology is performed on a real-world case study from Madrid. Actual rainfall data is used to obtain results comparable to that of the real-world operation. These results are presented from a model fitting perspective, but also from a control-oriented point of view.

2. METHODOLOGY

Within a MPC-based approach, the general optimal control problem can be posed by means of a state-space discrete-time model as follows:

$$\begin{aligned} \min_{\mathbf{x}(k), \mathbf{u}(k)} \quad & J(k) & (1a) \\ \text{s.t.} \quad & \mathbf{x}(k+1) = \mathbf{f}(\mathbf{x}(k), \mathbf{u}(k), \mathbf{w}(k)) & (1b) \\ & \mathbf{h}(\mathbf{x}(k), \mathbf{u}(k), \mathbf{w}(k)) \geq \mathbf{0}, & (1c) \\ & \mathbf{g}(\mathbf{x}(k), \mathbf{u}(k), \mathbf{w}(k)) = \mathbf{0}, & (1d) \\ & \mathbf{x}_{\min} \leq \mathbf{x}(k) \leq \mathbf{x}_{\max}, & (1e) \\ & \mathbf{u}_{\min} \leq \mathbf{u}(k) \leq \mathbf{u}_{\max} & (1f) \end{aligned}$$

where $\mathbf{x}(k)$ ¹ is the state vector, containing variables such as the tanks volumes, $\mathbf{u}(k)$ is the control input vector, containing variables representing the flows through actuators, and $\mathbf{w}(k)$ is the disturbance vector, related to rain runoff and intensity. The control-oriented model is set as a constraint of the problem through functions \mathbf{f} , \mathbf{h} and \mathbf{g} (with \mathbf{x}_{\min} , \mathbf{x}_{\max} , \mathbf{u}_{\min} and \mathbf{u}_{\max} being the physical limits of the system elements). These equations have to approximate the network behaviour while remaining simple, prioritizing linear and convex functions.

2.1 Simplified conceptual modelling

A number of typical network elements can be represented using basic hydraulic models.

Mass balance at junctions. A junction node is defined as the convergence point of two or more pipes. The mass balance equation relates its inflows and outflows as follows:

$$\sum_{i=1}^{n_{in}} q_i^{in}(k) = \sum_{j=1}^{n_{out}} q_j^{out}(k), \quad (2)$$

where q_i^{in} and q_j^{out} are respectively the inflow from the i -th pipe and the outflow through the j -th pipe, and n_{in} and n_{out} denote the total number of inflows and outflows.

Volume dynamics at the tanks Storage tanks temporarily retain polluted water, allowing partial control of the downstream flow. Their volume evolves as follows:

$$v(k+1) = v(k) + \Delta t \left(\sum_{i=1}^{n_{in}} q_i^{in}(k) - \sum_{j=1}^{n_{out}} q_j^{out}(k) \right), \quad (3a)$$

$$0 \leq q_i^{in}(k) \leq q^{in,max}, \quad (3b)$$

$$0 \leq q_j^{out}(k) \leq q^{out,max}, \quad (3c)$$

where v denotes the tank volume, q_i^{in} and q_i^{out} represent, in this case, the inflows and outflows of the tank (limited by $q^{in,max}$ and $q^{out,max}$), which are shaped through actuators, and Δt is the sampling time.

Combined sewer overflow CSOs release excess water into natural bodies when the physical or operational capacity of network components is surpassed:

- Storage tanks include an overflow mechanism to prevent volume from exceeding the maximum capacity v_{max} . This outfall can be modelled as:

$$q^{CSO}(k) = \frac{1}{\Delta t} \max(0, v(k+1) - v^{max}), \quad (4)$$

where $v(k+1)$ is defined through (3a) and v^{max} is the physical limit of the tank storage capacity.

- WWTPs and CSO points can overflow when the incoming flow exceeds their capacity. This overflow can be defined as:

$$q^{out}(k) = \min(q^{in}(k), q^{max}), \quad (5a)$$

$$q^{CSO}(k) = q^{in}(k) - q^{out}(k), \quad (5b)$$

where q^{in} and q^{out} are the flow upstream and downstream to the CSO point, respectively. Besides, q^{max} is the maximum capacity of the network element.

2.2 Data-driven modelling

However, some elements in an UDS may have complex dynamics which cannot be captured by simplified conceptual models, such as active components (e.g. pumps and valves) and standard elements with a complex behaviour under demanding conditions, like collectors running full during intense rainfall. In these cases, data-based models provide an effective alternative. The derivation of these models requires three key sources of information: (i) large volumes of input-output data from the component to model, covering a wide range of operating conditions; (ii) expert knowledge to guide the modelling process and define parametrized expressions consistent with the element's behaviour; (iii) data-fitting algorithms that identify patterns from the data, estimating the optimal parameter values.

Based on these requisites, a framework for deriving data-driven models can be defined. The preliminary step involves analysing the network to identify which components require data-driven modelling. Then, the following steps are applied to each selected element:

- (1) **The necessary input-output data are gathered**, considering multiple rain scenarios of different characteristics. Although measurements can be used if sensors are installed, input-output synthetic data is often generated through a high-fidelity detailed network hydrodynamics model under realistic conditions.
- (2) **The input-output data are graphically represented**, assigning each variable to an axis. In this

¹ Note that $k = t, t+1, \dots, t+H-1$ is the optimization time step, with t being the current time instant of the event, and H being the optimization horizon.

way, experts can analyse the element's behaviour, and the relation between inflows and outflows. For elements with multiple inputs/outputs, the analysis can be performed iteratively, considering different input/output pairs and studying the effect of each input over each output.

(3) **The insights from the data are used to select a mathematical expression** that can represent the component's behaviour. This includes deciding the type of function to be used and its parametrization:

- Certain mathematical functions are not desirable for optimization-oriented models because they may pose problems for convergence. Preferred expressions include (in decreasing order): (a) linear functions, (b) polynomial functions, (c) logarithmic functions, and (d) exponential functions.
- Moreover, a trade-off must be considered in the number of parameters, as excessive parametrization increases complexity and even may degrade the obtained solution.

(4) **A data-fitting algorithm is applied** to get the optimal set of parameter values. Various types of algorithms are described in Table 1, namely linear (LLS) and non-linear (NLLS) least squares (Hansen et al., 2013), non-parametric (Eubank, 1999), and heuristic fitting (Gulsen et al., 1995).

(5) **The obtained data-based equation is evaluated** over calibration and test rain scenario data, comparing real and predicted output values.

Flow-setpoint conversion In UDS, actuators are mainly associated with tank operations, namely *filling*, i.e., storing polluted water during rainfall; and *emptying*, i.e., releasing it when treatment facilities have sufficient capacity. These operations are usually executed through pumps (with adjustable curves) or orifices (with controllable aperture level). The tank dynamics, described in (3), depend on the inflows and outflows, which are assigned certain values within the MPC prediction to optimize the tank operation according to the cost function. Thus, these predicted flows must be converted into actuator setpoints for their application in the subsequent control step, leading approximately to the optimized flow targets. A similar procedure to that described earlier can be applied to derive the flow-setpoint conversion function, but various updates are required:

- I. The relationship between actuator inflows and outflows may be affected by additional factors modifying its operation, such as saturations during intense rainfalls. Thus, other network variables may have to be incorporated to the input-output datasets.
- II. When generating synthetic data, the full range of setpoint values must be tested to accurately reconstruct the actuator's behaviour. This is achieved by defining a discrete grid of setpoint values (e.g. orifice openings with fixed increments). To reduce computational cost, separate datasets can be obtained for each actuator, varying only the studied actuator while controlling others through expert-based rules.
- III. The generated data must be grouped into batches, depending on the specific actuator value, allowing the analysis of each specific actuator configuration independently. This helps to understand the shape of the function that best models the actuator behaviour

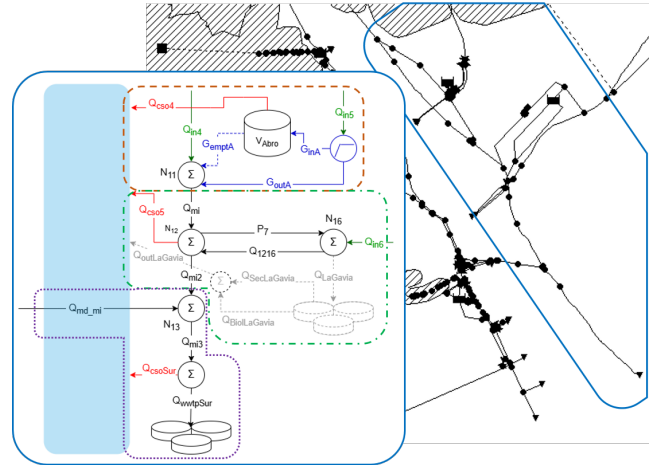


Fig. 1. Schematic representation of the simplified model of the left bank, depicted over the detailed model.

depending on the setpoint value. Such analysis would require to compare the flow related to the control action against all the other involved variables.

We must remark that a conversion function is derived for each discrete setpoint value of each actuator. During application, the input variables for the conversion function are obtained from the optimized results (at the next prediction step), and the conversion functions for all the setpoints are applied over them. The obtained values are then compared against the optimized value for the actuator flow variable (normally its outflow). The final setpoint value is selected depending on a pre-defined criterion, such as choosing the discrete setpoint value that provides the closest conversion function value to the optimized value, or even interpolating a setpoint value between the lower and upper discrete setpoint values.

3. CASE STUDY

The proposed methodology is assessed using a case study implemented on a fraction of Madrid's city UDS. Specifically, we use a reduced part of the network, mainly composed of two interceptors, parallel to the Manzanares river by its left and right margins (i.e., LM and RM), where the filling and emptying of two tanks are regulated using actuators. The main properties of this pilot are summarised in Table 2. A detailed UDS model was implemented using Storm Water Management Model (SWMM) (Rossman and Huber, 2015). This model includes the section considered as pilot, but also the rest of the UDS, which generates the inflows to the actual pilot. Note that actuators outside the pilot are controlled by pre-defined rules.

4. RESULTS AND DISCUSSION

The evaluation of the modelling framework is carried out from data-fitting and control-oriented perspectives. Although a simplified model was obtained for the complete pilot with its two margins, for the sake of simplicity, we focus here on LM, whose graphical representation is shown over the detailed model in Fig. 1.

Table 1. Data-fitting algorithms: (i) LLS, (ii) NLLS, (iii) non-parametric and (iv) heuristic.

Use		Advantages	Limitations
(i)	Linear parametrized models	Extremely efficient, with closed-form solution	Non-linear systems, outliers and noise
(ii)	Non-linear parametrized models	Robust, works for numerous classes of models	May be costly or non-optimal
(iii)	Unknown function form	Flexible, minimal assumptions on expressions	Risk of overfitting, loss of expert insight
(iv)	Non-smooth objective	May avoid local minima, derivative-free	Computationally costly, time-consuming

Table 2. Characteristics of the case study UDS

Element	Nº	Characteristics
Tank	2	Butarque [RM, $3 \cdot 10^5 m^3$ max. capacity (MC)], Abroñigales [LM, $2 \cdot 10^5 m^3$ MC]
WWTP	3	Butarque (RM) and Sur (LM), total $4.75 \cdot 10^5 m^3/day$ MC; La Gavia (LM)
Inlets	7	4 in RM and 3 in LM
CSOs	6	3 in RM and 3 in LM

4.1 Modelling

The LM model can be divided into three main areas: upstream LM and Abroñigales tank (dashed enclosure in Fig. 1), La Gavia WWTP area (dashed-dotted enclosure), and RM - LM connection and Sur WWTP area (dotted enclosure). The model equations are presented in Table 3, using the variable names in Fig. 1.

Upstream LM and Abroñigales tank This section contains two of the water inlets within LM. Firstly, the upstream flow to LM arrives through Q_{in4} , reaching virtual node² N_{11} , which also receives water from the Abroñigales tank outflow (G_{emptA}) and bypass (G_{outA}), yielding Q_{mi} (eq. (6)). Secondly, the water coming through Q_{in5} reaches the diversion point between Abroñigales tank inflow (G_{inA}) and bypass, where this division is controlled using an actuator (orifice) (eq. (7)). Abroñigales tank volume evolves depending on its inflows and outflows, physical/operational limits and related CSO (eqs. (8-10)).

La Gavia WWTP area The last water inlet is Q_{in6} , whose flow is passively divided into water bypassed downstream (Q_{1216}) and water conveyed to La Gavia WWTP area. The relationship between Q_{in6} and Q_{1216} was modelled using data-fitting due to its complexity, which cannot be properly represented using mass conservation only (eq. (11)). Then, we apply mass balance in N_{16} , regarding the physical limit to La Gavia inflow (eq. (12)). This flow is divided into the water receiving biological or secondary treatments, as well as the WWTP outfall (eqs. (13-15)). Next, two data-based equations are generated from N_{12} , using Q_{1216} and the flow upstream (Q_{mi}) to yield the flow downstream (Q_{mi2}) and the remaining portion of Q_{CSO5} , added to La Gavia outfall to yield the complete CSO flow (eqs. (16-18)). Finally, pump P_7 is modelled through a pair of data-based equations: the first converts the flows related to N_{12} into a “virtual” water level (eq. (19)), and the second mimics the actual pumping curve, which converts node level into pumped flow (eq. (20)).

RM-LM connection and Sur WWTP area This final part of LM is defined by the operation of Sur WWTP. The water conveyed through Q_{mi2} is added to the water coming from RM (eq. (21)) and then Sur WWTP’s inflow

² Virtual nodes are simplifications of actual connections in the detailed model, used to represent the flow balance.

is defined by its capacity, with the rest of incoming water being released as CSO (eqs. (22-23)).

Discussion From a modelling perspective, we can evaluate the goodness of fitting of the data-based equations, namely (11, 16, 17, 19, 20) in Table 3. To calibrate them, outflow and inflow/s data are gathered from available rain events, which are shown in Table 4. Besides, all potential setpoint combinations must be considered. We define 10% opening step in each actuator, leading to a total of 100 scenarios per rain, considering the two available actuators (i.e., orifices associated to G_{outA} and G_{emptA}).

Data-fitting performance metrics are presented in Table 5, namely root-mean squared error ($RMSE$), mean absolute error (MAE) and coefficient of determination (R^2). The first two provide error measures in flow units (m^3/s), with the former being more affected by outliers, showing if there are occasional large errors; and the latter being more robust, increasing interpretability. R^2 measures how well the model explains the variance in data. The mean, standard deviation and maximum value of the true outcome of each expression are also given in order to enrich the analysis.

Analysing Table 5, we can appreciate how each expression excellently fits the associated input-output data. All the data-based models have $R^2 > 0.9$, with small errors in comparison to the mean values. Regarding the resulting values, (16) would be the expression with the most limited performance, although its metrics remain satisfactory. (11) and (19) stand out due to their notable capabilities.

4.2 Control

The data-fitting results can be complemented with the MPC control performance under a realistic rain scenario. Besides, this scenario can be used to evaluate the flow-setpoint conversion functions for the two actuators included within the case study, defined by the filling and emptying operations of Abroñigales.

Filling operation The inflow to the tank is defined in (7). The actuator setpoint is the opening level of the associated orifice, with 0% implying that the bypass G_{outA} is closed. Thus, a function converting Q_{in5} into G_{outA} must be defined, namely:

$$G_{outA}(t) = \begin{cases} m_i (Q_{in5}(t) - x_i) + y_i, & Q_{in5}(t) < p_i \\ f_2(Q_{in5}, a_i, b_i, c_i, d_i, e_i), & \text{otherwise} \end{cases} \quad (24)$$

where $f_2(Q_{in5}, a_i, b_i, c_i, d_i, e_i) = a_i Q_{in5}^2(t) + b_i Q_{in5}(t) + c_i + d_i (\ln(e_i Q_{in5}(t)))$, with parameters depending on i because they belong to a different potential setpoint value on the defined grid (with a step of 10%). The equation represents two distinct modes: (i) a linear expression, describing the behaviour when the bypass can accommodate the

Table 3. Summary of the simplified model of LM, indicating each equation's description, type (SC = simplified conceptual, DB = data-based), and formula.

Description	Type	Equation
<i>Upstream LM and Abroñigales tank</i>		
Mass balance in N_{11}	SC (2)	$Q_{mi}(t) = Q_{in4}(t) + G_{emptA}(t) + G_{outA}(t)$ (6)
Tank inflow and bypass from Q_{in5}	SC (2)	$G_{inA}(t) = Q_{in5}(t) - G_{outA}(t)$ (7)
Abroñigales tank volume dynamics	SC (3a)	$V_{Abro}(t+1) = V_{Abro}(t) + \Delta t (G_{inA}(t) - G_{emptA}(t) - Q_{CSO4}(t))$ (8)
Abroñigales tank outflow limit	SC (3c)	$0 \leq G_{emptA}(t) \leq V_{Abro}(t)/\Delta t$ (9)
Abroñigales tank associated CSO	SC (4)	$Q_{CSO4}(t) = \max(0, V_{Abro}(t+1) - V_{Abro}^{max})/\Delta t$ (10)
<i>La Gavia WWTP area</i>		
Computation of Q_{1216} from Q_{in6}	DB	$Q_{1216}(t) = \max(0, 0.003Q_{in6}^2(t) + 0.921Q_{in6}(t) - 0.538)$ (11)
Mass balance in N_{16} (max. outflow)	SC (2,5a)	$Q_{LaGavia}(t) = \min(1.5, P_7(t) + (Q_{in6}(t) - Q_{1216}(t)))$ (12)
Biological treatment in La Gavia	SC (5a)	$Q_{BiolLaGavia}(t) = \min(1.25, Q_{LaGavia}(t))$ (13)
Secondary treatment in La Gavia	SC (2)	$Q_{SecLaGavia}(t) = Q_{LaGavia}(t) - Q_{BiolLaGavia}(t)$ (14)
Flow to CSO from La Gavia	SC (2)	$Q_{outLaGavia}(t) = Q_{SecLaGavia}(t) - Q_{BiolLaGavia}(t)$ (15)
Downstream from N_{12}	DB	$Q_{mi2}(t) = -0.003Q_{1216}^2(t) - 0.041Q_{mi}^2(t) + 0.167Q_{1216}(t) + 0.874Q_{mi}(t)$ (16)
CSO discharge from N_{12}	DB	$Q_{CSO5.1}(t) = 0.006Q_{1216}^2(t) + 0.042Q_{mi}^2(t) + 0.707Q_{1216}(t) + 0.155Q_{mi}(t)$ (17)
Computation of Q_{CSO5}	SC (2)	$Q_{CSO5}(t) = Q_{CSO5.1}(t) + Q_{outLaGavia}(t)$ (18)
N_{12} water level from flows	DB	$L_7(t) = -0.254Q_{mi2}(t) - 0.6Q_{CSO5}(t) + 0.583Q_{1216}(t) + 0.77Q_{mi}(t) + 0.868$ (19)
Pump P_7 level-to-flow curve	DB	$P_7(t) = 0.455/(0.883 + e^{-65.998L_7(t)+77.339}) + 0.132$ (20)
<i>RM-LM connection and Sur WWTP area</i>		
LM downstream flow	SC (2)	$Q_{mi3}(t) = Q_{mi2}(t) + Q_{md_mi}(t)$ (21)
Flow entering Sur WWTP	SC (5a)	$Q_{WWTPSur}(t) = \min(6, Q_{mi3}(t))$ (22)
CSO from Sur WWTP	SC (5b)	$Q_{CSOSur}(t) = Q_{mi3}(t) - Q_{WWTPSur}(t)$ (23)

Table 4. Precipitation P (mm), maximum intensity I_{max} (mm/h), date and duration of the calibration rains scenarios

P	I_{max}	Date	Duration
17.0	31.2	2016-10-22	10h 10min
35.8	76.8	2017-01-09	17h 20min
23.6	50.4	2017-02-07	5h 35 min
15.4	33.6	2017-12-12	3h 50 min
21.3	36.0	2018-03-04	13h 45 min
19.4	60.0	2018-03-10	1h 5 min

Table 5. Summary of model performance metrics.

Eq.	$\bar{y} \pm \sigma(y)$	max(y)	RMSE	MAE	R^2
(11)	3.28 ± 5.01	21.26	0.44	0.21	0.99
(16)	4.18 ± 1.41	7.54	0.39	0.32	0.92
(17)	6.86 ± 6.55	27.83	0.95	0.51	0.97
(19)	3.61 ± 1.19	5.61	0.09	0.06	0.99
(20)	0.64 ± 0.05	0.65	$9 \cdot 10^{-3}$	$4 \cdot 10^{-3}$	0.97

water coming from Q_{in5} ; and (ii) a saturation expression, representing system overload at the diversion node (with the rest of water entering the tank). The parameter values and discontinuity points of are given in Table 6.

Emptying operation The outflow of the tank depends on factors such as the tank water level (D_{Abro}) and other flows related to (6), namely Q_{in4} and G_{outA} . In this case, the actuator setpoint is the opening of the associated orifice, which is directly related to G_{emptA} , and the conversion function relates the mentioned factors with this flow:

$$G_{emptA}(t) = f_i D_{Abro}^2(t) + g_i D_{Abro}(t) + h_i G_{outA}(t) + r_i Q_{in4}(t) + s_i, \quad (25)$$

where the parameter values are showed in Table 6.

Discussion To evaluate the goodness of conversion functions, we have implemented them within a close-loop

framework, testing the complete control scheme and the derived model (including the RM model). The role of the virtual reality is played by the SWMM detailed model, whereas the MPC problem is solved using General Algebraic Modelling System or GAMS (GAMS Development Corporation, 2024), which is a high-level modelling software that allows to solve linear, non-linear, and even mixed-integer optimization problems. In this case, the control-oriented model is implemented as the constraints in (3), and the cost function J has three sub-objectives: J_{CSO} , which seeks to minimize the CSO volume; J_{WWTP} , which tries to maximize WWTP utilization; and J_{smooth} , which seeks to minimize changes in the actuator setpoints.

The methodology is tested on a rain scenario occurred on 12/10/2024, with a duration of 11 hours and 21.9 mm of precipitation. The conversion functions are assessed by comparing predicted and actual actuator flows. Note that, during application, the input variables for each function are extracted from the optimization results (at $k = t + 1$), and the conversion functions for all the potential setpoints are applied over them. The obtained values are compared against G_{outA} and G_{emptA} , and the setpoints whose conversion function lead to the closest outcomes to the optimized value are selected, interpolating the final setpoint value between the lower and upper discrete setpoint values. Thus, in Fig. 2, we compare the MPC predicted flow for G_{outA} and G_{emptA} with the actual flow value at the associated SWMM link at the next time instant (when the final setpoint is actually applied). Both SWMM and GAMS lines are extremely similar, denoting the excellent conversion capability of (24) and (25). The R^2 metric in the estimation is 0.98 for G_{outA} and a 0.99 for G_{emptA} , showing their outstanding performance.

Finally, to illustrate the advantages of deriving accurate control-oriented model and conversion functions, the overall controller performance in the considered rain event is assessed by comparing the CSO discharges and WWTP

Table 6. Parameter values and discontinuity points for (24) and (25).

i	0	1	2	3	4	5	6	7	8	9	10
%	0	10	20	30	40	50	60	70	80	90	100
m_i	0	0.59	0.93	0.94	1.04	1.05	1.10	1.10	1.06	1.09	1.08
x_i	0.26	0.26	0.26	0.26	0.26	0.26	0.26	0.26	0.26	0.26	0.26
y_i	0.10	0.10	0.17	0.21	0.24	0.26	0.26	0.26	0.26	0.26	0.26
p_i	0	0.90	1.10	1.50	1.80	2.20	2.50	2.90	3.40	3.65	4.00
a_i	0	$5 \cdot 10^{-6}$	$3 \cdot 10^{-5}$	$-2 \cdot 10^{-5}$	$-9 \cdot 10^{-5}$	$-2 \cdot 10^{-4}$	$-9 \cdot 10^{-5}$	$-2 \cdot 10^{-4}$	$-6 \cdot 10^{-4}$	$-3 \cdot 10^{-4}$	$8 \cdot 10^{-6}$
b_i	0	$6 \cdot 10^{-4}$	$6 \cdot 10^{-4}$	$4 \cdot 10^{-3}$	$8 \cdot 10^{-3}$	$1 \cdot 10^{-2}$	$9 \cdot 10^{-3}$	$2 \cdot 10^{-2}$	$4 \cdot 10^{-2}$	$2 \cdot 10^{-2}$	$-7 \cdot 10^{-3}$
c_i	0	0.40	0.84	1.32	1.86	2.18	6.10	2.86	3.13	11.20	21.19
d_i	0	0.01	0.02	0.04	0.03	0.03	0.08	0.05	$-8 \cdot 10^{-3}$	0.20	0.42
e_i	0.3	$5.3 \cdot 10^3$	$1.5 \cdot 10^2$	1.80	0.18	9.50	0	64.1	0	0	0
f_i	0	-0.00	-0.01	-0.02	-0.03	-0.03	-0.04	-0.05	-0.06	-0.04	-0.05
g_i	0	0.12	0.30	0.47	0.62	0.78	0.93	1.09	1.25	1.11	1.29
h_i	0	-0.02	-0.04	-0.07	-0.10	-0.12	-0.15	-0.18	-0.20	-0.23	-0.27
r_i	0	-0.02	-0.03	-0.05	-0.07	-0.10	-0.13	-0.17	-0.21	-0.24	-0.28
s_i	0	0.24	0.29	0.36	0.46	0.56	0.66	0.78	0.88	1.66	1.71

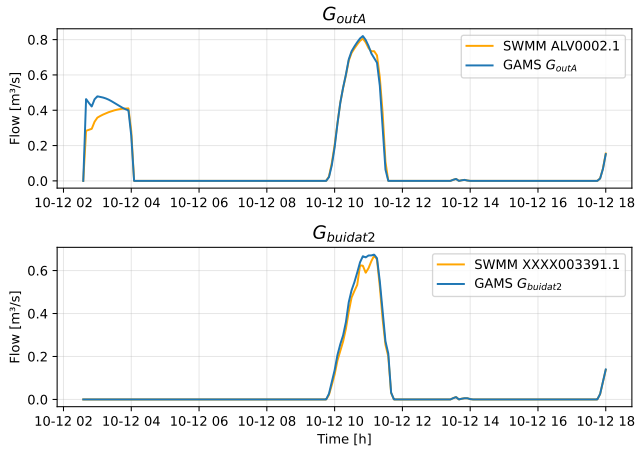


Fig. 2. Evolution of the actuator-related flows G_{outA} and G_{emptA} on the 12/10/2024 event.

inflows for the elements in LM. These values are presented in Table 7 for the MPC method, as well as a RBC system. The results show how the MPC controller is able of notably reducing the CSO spillage in LM, specifically by a 19.1%; while increasing the WWTP inflow by a 7.9%.

Table 7. Summary of key performance indicators for RBC and MPC.

	RBC ($10^3 m^3$)	MPC ($10^3 m^3$)
Q_{CSO4}	0	0
Q_{CSO5}	313.09	238.19
Q_{CSOSur}	74.06	74.96
$Q_{WWTPSur}$	240.45	259.43

5. CONCLUSION

This article presents a control-oriented modelling framework for UDS, focused on data-based models. The methodology defines a guide to generate data-driven expressions that represent the complex behaviour of network elements using input-output data, expert knowledge and data-fitting. Moreover, the derivation and application of flow-setpoint conversion functions for actuators are presented.

The methodology is assessed in a realistic pilot from Madrid, Spain. A control-oriented model and conversion functions are derived, evaluating them using a real-world

rain scenario over virtual reality. The results show high accuracy of the data-based models, as well as significant improvements in terms of discharge reduction and WWTP usage by using these models and functions in MPC.

In future work, we plan to explore state-of-the-art modelling techniques, such as Dynamic Mode Decomposition (DMD), to retrieve linear models from input-output datasets, reducing model complexity and dependence on expert knowledge, yielding convex MPC formulations, increasing computational efficiency.

DECLARATION OF GENERATIVE AI AND AI-ASSISTED TECHNOLOGIES IN THE WRITING PROCESS

During the preparation of this work the author(s) used ChatGPT in order to receive wording suggestions. After using this tool/service, the author(s) reviewed and edited the content as needed and take(s) full responsibility for the content of the publication.

REFERENCES

- Aulinas, M., Nieves, J.C., Cortés, U., and Poch, M. (2011). Supporting decision making in urban wastewater systems using a knowledge-based approach. *Environmental Modelling & Software*, 26(5), 562–572.
- Eubank, R.L. (1999). *Nonparametric regression and spline smoothing*. CRC press.
- GAMS Development Corporation (2024). *GAMS - The Solver Manuals*. GAMS Development Corporation, Washington, DC, USA.
- Gulsen, M., Smith, A., and Tate, D. (1995). A genetic algorithm approach to curve fitting. *International Journal of Production Research*, 33(7), 1911–1923.
- Hansen, P.C., Pereyra, V., and Scherer, G. (2013). *Least squares data fitting with applications*. JHU Press.
- Joseph-Duran, B., Ocampo-Martinez, C., and Cembrano, G. (2015). Output-feedback control of combined sewer networks through receding horizon control with moving horizon estimation. *Water Resources Research*, 51(10), 8129–8145.
- McGrane, S.J. (2016). Impacts of urbanisation on hydrological and water quality dynamics, and urban water management: a review. *Hydrological Sciences Journal*, 61(13), 2295–2311.

Mullapudi, A., Lewis, M.J., Gruden, C.L., and Kerkez, B. (2020). Deep reinforcement learning for the real time control of stormwater systems. *Advances in water resources*, 140, 103600.

Rossman, L. and Huber, W. (2015). Storm water management model reference manual volume I, hydrology. US EPA Office of Research and Development, Washington, DC. Technical report, EPA/600/R-15.

UN-Water (2017). The United Nations World Water Development Report 2017. Wastewater: The Untapped Resource.